COST Action TU1202:

Short Term Scientific Mission Report

STSM Participants: Dr Ross Stirling, Ross.Stirling@ncl.ac.uk
Miss Rosalind Hen-Jones, R.Hen-Jones@ncl.ac.uk
Newcastle University (UK)
STSM Topic: Investigating geotechnical/geophysical relationships in unsaturated glacial till
Host: Prof. Yu-Jun Cui, École des Ponts ParisTech (FR), Yujun.Cui@enpc.fr
Period: 02/02/2015 to 22/02/2015

1. Summary

The purpose of the mission was to learn new techniques in the determination of small-strain shear stiffness, measurement of suction and thermal conductivity. Additionally, on-going research into the development of cracking during repeated wetting and drying using a purpose built environmental chamber was observed. Although the mission was relatively short in duration, the varied experimental programme allowed the three main relationships to be established along the initial drying path. Each dataset not only corroborates and informs the interpretation of the others but is extremely useful in combining with ongoing research at the grant holder's home institution. The results have been discussed with the mission host and there is strong potential for collaborative further work and publication on the effects of the drying mechanism on geophysical and geotechnical properties.

2. Soil used

The soil studied was derived from a glacial till deposit in County Durham, UK and has been the focus of ongoing research into the effects of climate change on infrastructure slope stability at the BIONICS embankment facility (Northumberland, UK). The material was shipped to the host institution in a dried, crushed and sieved state ahead of the STSM start date. Some basic properties of the material are provided in Table 1. All testing was conducted on material wetted to 22% and sealed in plastic bags for a period of 24 hours prior to sample formation.

Table 1 Basic soil properties of BIONICS material.

Property		Value
Plasticity Index, I_p (%)		16
Plastic limit, w_p (%)		17
Liquid limit, w_L (%)		33
Specific gravity, G_S		2.64
In situ dry density (Mg/m^3)		1.65
Compaction water content (%)		22
Maximum soil aggregates size (mm)		5.00
PSD	Cu	9.6
	Cz	1.2

3. Activities

Three main activities were undertaken during the STSM. A brief description of the methods and techniques learned is provided, followed by presentation of the main results.

3.1 SWRC by Chilled Mirror Dewpoint Technique

A Decagon Devices WP4 was used to rapidly (5-10 min) measure soil-water potential within the range 0 to -300 MPa with a resolution of 0.1 MPa. This method determines the relative humidity of the air above a sample in a closed chamber where at temperature equilibrium, relative humidity is a direct measurement of water potential (Decagon Devices Inc., 2015).

Samples were statically compacted at a rate of approx. 0.3 mm/min to a diameter of 38 mm and height 8 mm. The final load was maintained for 20 min to allow for pore pressure dissipation and minimise post-compaction swelling. Samples were then sealed for 24 hours to equilibrate. In order to populate a useful portion of the SWRC (AEV and subsequent desaturation), samples were dried to intended masses corresponding to a range of water contents (Figure 1a). On achieving the desired mass, the sample was then divided. A portion was placed into the drawer of the WP4 after being left to reach temperature equilibrium with the device for no less than 15 min. The remaining portion was used for bulk density determination. By weighing in air and in a non-wetting fluid of known density, the bulk density of the sample may be deduced (Figure 1b). This enabled the calculation of volumetric water content from the bulk density of the soil at known gravimetric water content and that of water, this also enables the degree of saturation to be defined.

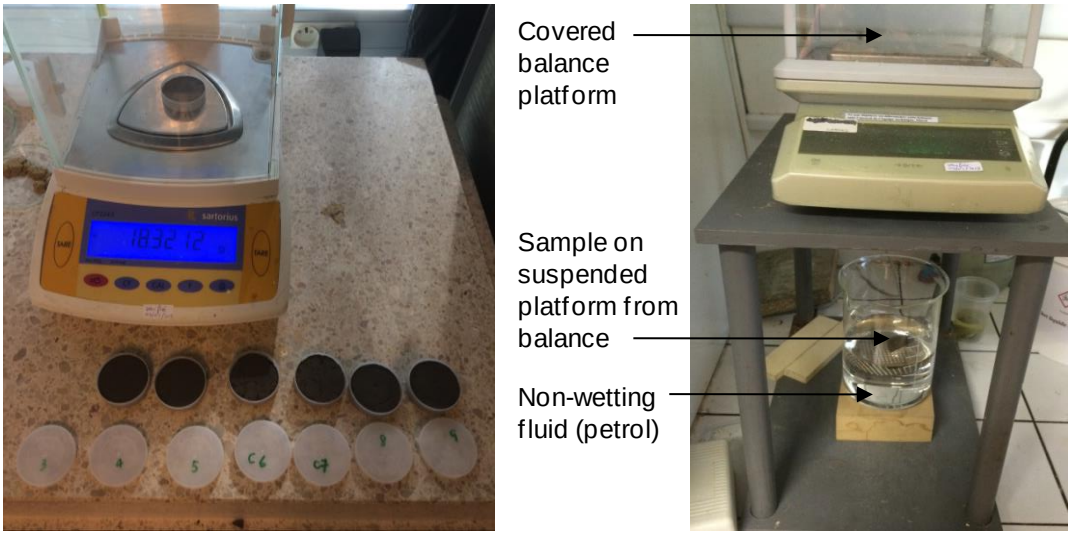

Figure 1 (a) WP4 samples drying to predetermined masses/moisture contents and (b) determination of sample density apparatus.

3.1.1 Results

The drying curve was established in most detail, followed by a wetting curve as presented in Figure 2. The general shape of the drying curve is as would be expected with an AEV of approximately 600kPa and subsequent de-sorption to a residual of Sr 20%. Similarly, the re-wetting curve shows a classic, shallower sorption path including a reduced achievable saturation after wetting due to entrapped air.

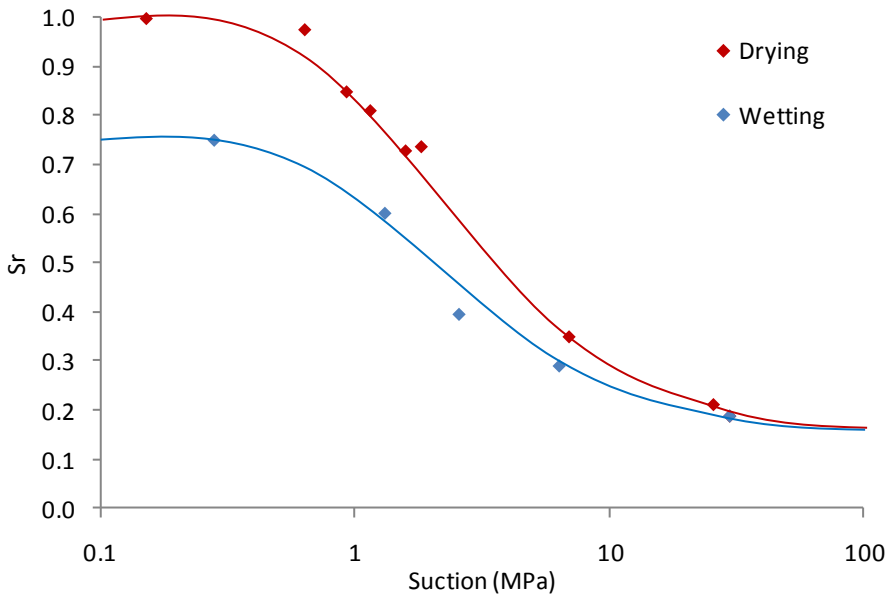

Figure 2 SWRC for initial drying and single wetting path

As mentioned previously, the soil tested has been the focus of numerous investigations, principally at Newcastle and Durham Universities. This has allowed the newly acquired data from the activities of the STSM to be compared with that of other techniques using similar sample preparation and properties. Figure 3 shows the new data overlaid upon data gained using the filter paper technique (Noguchi et al. 2011 cited in Mendes and Toll 2013). An excellent agreement between the datasets is found with a good correlation of AEV.

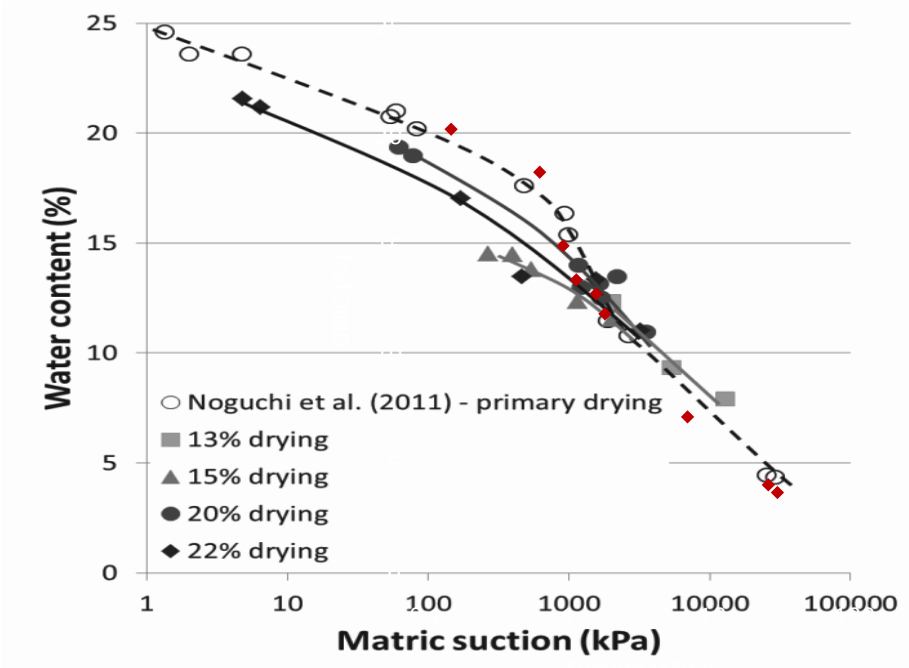

Figure 3 New - existing SWRC overlay

3.2 Measurement of thermal conductivity

The thermal conductivity of two identical samples was measured using a Decagon Devices KD2 Pro probe via a stage drying process. The instrument uses the transient line heat source technique and resolves thermal conductivity to within ±10%. Samples were statically compacted to 50 mm diameter and 120 mm height at 22% water content and ~1.65 Mg/m^3. After a 24 hour sealed equalisation period, the samples were drilled with a 2.5mm bit to the probe length of 100 mm. The probe-sample dimensions were selected according to the manufacturer's recommendation of at least a 20 mm radius about the probe to avoid boundary effects. Samples were kept in the temperature and humidity controlled Navier laboratory to maintain consistency in thermal conditions between readings.

Samples were sealed for 24 hours between drying stages. Upon each water content range being reached (as determined by mass balance), the probe was coated in thermally conductive grease and inserted into the sample as shown in Figure 4a. This grease is shown to line the tested hole through the centre of the sample on the penultimate day of testing in Figure 4b. Three tests were conducted at each drying stage at 15 minute intervals due to the nature of the technique raising the internal sample temperature. An average thermal conductivity and average bulk mass from weighing pre- and post- testing is reported. Sample dimensions were measured using callipers but negligible shrinkage was observed within the accuracy of the measurement method.

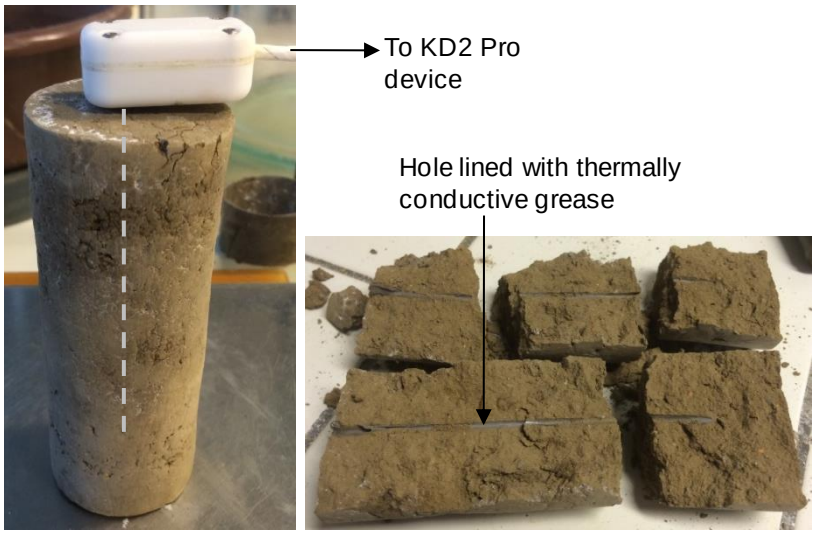

Figure 4 Thermal conductivity testing setup (a) probe inserted into relatively dry, intact sample and (b) sample broken for moisture determination showing lined hole.

3.2.1 Results

The thermal conductivity of the material at decreasing water content is presented in Figure 5. Thermal conductivity was found not to change during drying from the 'as compacted' content until the range of 13-15% gravimetric water content. This is considered to coincide with the entry of air (as determined in the SWRC - Figure 3) and the beginning of rapid desaturation, beyond which thermal conductivity was found to decrease considerably. As concluded by Tang et al. (2008), the decrease in thermal conductivity of a drying clay is almost directly proportional to the increase in the volume fraction of air, as opposed to the fraction of soil or water. Hence, it is reasonable to expect that the measured thermal conductivity data presented show the greatest change for the drying stages after air entry.

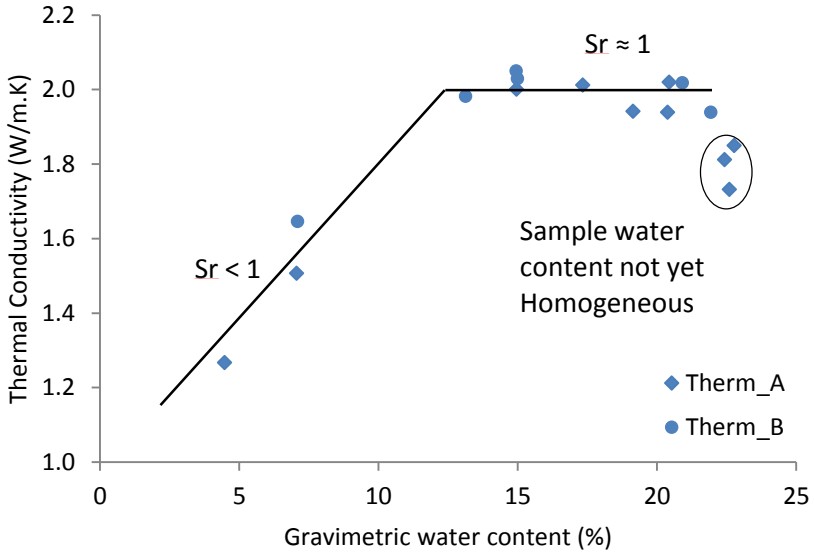

Figure 5 Thermal conductivity measurements at reducing sample masses due to drying

3.3 Determination of small-strain stiffness

The small-strain shear stiffness (G_{max}) was measured via Bender Elements. This technique uses S-wave propagation to infer the shear modulus of a given medium using the shear wave velocity ($V_s = l/\Delta t$) and the bulk density (ρ) according to $G_{max} = \rho V_s$. As with the previous tests, samples were prepared at 22% to ~1.65 Mg/m^3 using static compaction. Research conducted at ENPC showed 1:1 sample dimensions to be most consistent and so a diameter and height of 50 mm was selected. The elements themselves were sealed within platens and protrude approximately 2 mm and are 10 mm long. In order to ensure maximum element-soil contact, impressions were made in the sample ends as shown in Figure 6a. Three corresponding pairs of grooves were carefully positioned as the relative transmitting and receiving element orientation must be parallel.

Upon samples reaching the required water content and having undergone a 24 hour period of equalisation, samples were positioned between the element platens and manually restrained. At each water content, the elements were excited at the three positions in turn and weight prior and after testing. Three samples were tested by staged drying. At each phase of testing, both P- and S-wave transmission across element to element contact was recorded for the purposes of calibration and system verification.

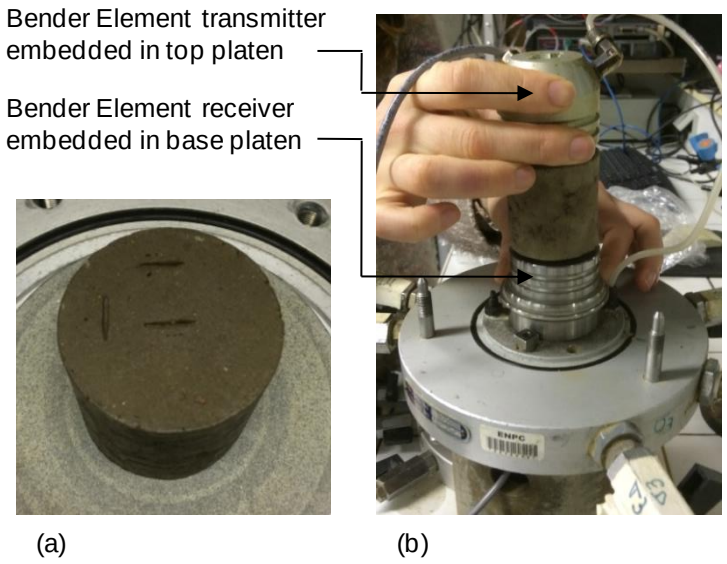

Figure 6 Bender Element experimental setup (a) sample showing three element impressions and (b) sample positioned between platens during testing.

3.3.1 Results

The G_{max} results presented in this report are strictly preliminary and it must be appreciated that a significant period of post-processing is required in the use of Bender Elements to ensure reliable data interpretation. The greatest difficulty experienced in the use of this technique is the confident identification of s-wave arrival. The waveform presented in Figure 7 illustrates the most easily identifiable s-wave arrival using the peak-to-peak approach, although other methods are extensively discussed in the literature.

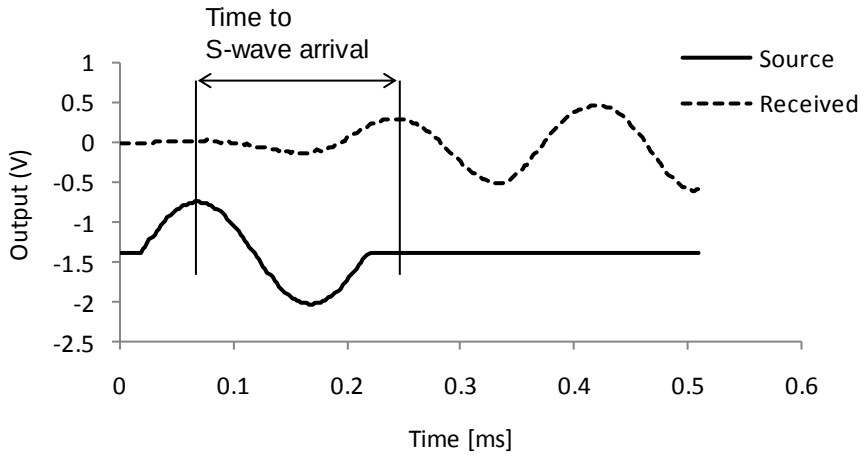

Figure 7 Example S-wave response at *w* = 12%.

To enable the rapid, preliminary analysis of recorded data, the GDS Instruments Excel add-in 'BEAT' (Bender Element Analysis Tool) was used. This has provided the G_{max} data presented in Figure 8, although it must be emphasised that the automated 'picking' of s-wave arrival time does require further confirmation manually. However, a general increase in shear modulus is observed despite a relatively large field of scatter. Importantly, G_{max} is found to decrease considerably at very low water contents and this is considered a function of the increased development of fracturing at the micro-structural level. Such features reduce the ability of the soil to propagate s-waves and indicate the reduction of stiffness at small-strain. Research at the home institution is already underway to investigate this mechanism via a series of methods including E-SEM, XRCT and resistivity.

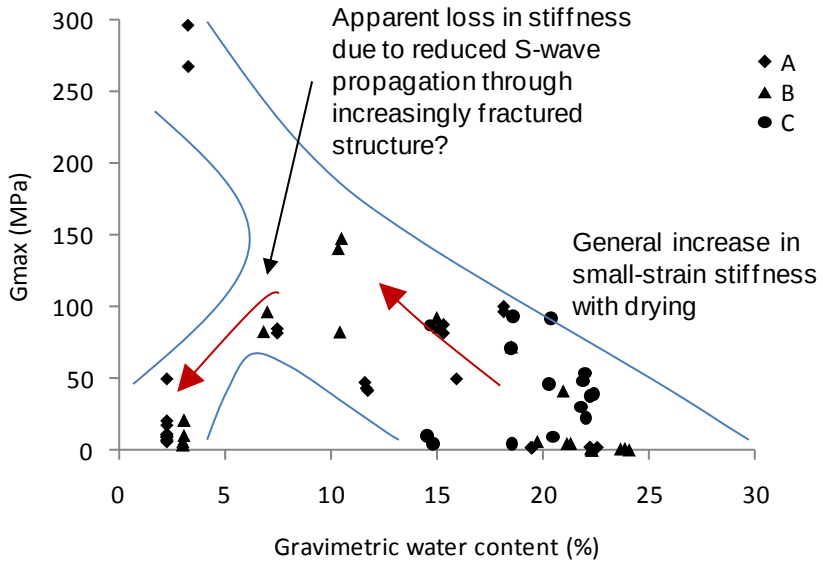

Figure 8 Small-strain shear modulus change with drying.

4. Acknowledgments

The STSM participants would like to thank Professor Yu-Jun Cui for hosting the STSM and not only for providing access to the excellent facilities at ENPC but for his encouragement in the work and continued collaboration. Additionally, appreciation is extended to the following researchers and technicians for their help and generosity: Dr Anh Minh Tang, Dr Chao-Sheng Tang, Dr Lingling Zeng, Mr Emmanuel De Laure and Ms Marine Lemaire.